DIRECTIONAL ANTENNA CHANNEL MODELING IN URBAN AREA USING RAY TRACING

Zhuyin Li[1], Sithamparanathan Kandeepan[1], Andrea Giorgetti[2], Akram Al-Hourani[1], Kagiso Magowe[1]
[1]School of Engineering, RMIT University, Melbourne, Australia, [2]DEI, University of Bologna, Italy

Abstract – *Directional antennas are regarded as one of the key technologies to achieve higher signal quality and data rate. Evidence has shown that the directional antenna channel features can be very different from the omnidirectional ones. Therefore, it is essential to characterize the directional antenna channel model (DACM), since an accurate, easy-to-implement DACM plays a vital role in the wireless network design, optimization and utilization. In this paper, we cluster the incident rays based on the azimuth direction of arrival at the receiver and extract the features concerning the number of clusters, the distribution of the cluster center and the cluster power ratio. The proposed DACM is derived by the ray tracing method and is feasible for a typical urban scenario within a range of a few hundred meters. Moreover, our proposed model is verified by both ray tracing and numerical simulations. In this paper, we present the model derivation methodology, recommend the model parameters and offer an implementation guideline.*

Keywords – Directional channel modeling, direction of arrival, multipath clustering, radio propagation, ray tracing

1. INTRODUCTION

5G networks are born with the tags of high capacity, high energy efficiency and high data rate. In the last decades, multiple-input-multiple-output (MIMO) has been regarded as one of the most promising techniques to enable some of the 5G vital features [1]. Directional antennas can improve propagation quality by focusing the beam within some desired direction. We can, therefore, achieve longer transmission distance with higher performance and lower interference by enhancing the signal strength in the specific direction and suppressing the signal in other directions [2]. For instance, higher frequency bands above 6 GHz e.g. millimeter-wave (mmWave), as part of the 5G spectrum offer huge bandwidth, but at the same time, bring problems like high path loss, high penetration loss, limited delay spread and reflection dominated propagation [3]. Therefore, directional antennas are deployed to overcome such challenges. On the other hand, the utility of directional antennas at both traditional and higher frequency bands can bring new challenges to the wireless network design, development and implementation, with the increasing demand for the accuracy of the channel modeling [4]. Moreover, the angular information such as direction of arrival (DOA) and direction of departure (DOD), cannot be neglected in directional channels, because they are not only important features for the propagation model, but also affect other parameters like path loss and delay [5]. As a result, the traditional omnidirectional channel models cannot accurately estimate a directional antenna propagation.

Channel models are essential for wireless network design and analysis, since they give insights into the characteristics of the radio channel without conducting field measurements, which are usually time-consuming and costly. Among all the channel modeling methods, ray tracing, as a geometry-based technique, can provide an accurate estimation of the radio propagation with high computational speed [6]. In a ray tracing simulation (RTS), the software estimates possible paths between the transmitter and the receiver depending on the environment, and offers a list of outputs including path loss, DOA, DOD, delay etc. Furthermore, even though the RTS can offer a great number of multipath components (MPCs), it is not necessary to deal with MPCs individually. Many measurements have revealed that MPCs can be grouped into clusters with similar features such as DOA, DOD or delay. Such cluster-based channel models are more compact and intuitive since the intra-cluster, and inter-cluster statistics can be treated separately [7].

Considering the urge to have an accurate channel model in a directional propagation environment, we propose a directional antenna channel model (DACM) and also offer a generic methodology framework for channel modeling. In this paper, our main contributions can be summarized as follows: 1) We derive a clustering DACM using the ray tracing method. The model is feasible for a typical urban scenario in which the transmitter and the receiver are a few hundred meters apart, such as an urban microcell network. 2) We cluster the MPCs based on the azimuth DOA, and further extract the probability mass function (PMF) of the number of clusters, the probability density function (PDF) of the azimuth cluster center and the cluster power ratio. 3) The derived PDF expressions are simple functions of only a few distance-independent parameters.

The remainder of the paper is organized as follows. In section 2, a literature review on the existing directional channel model is presented. We also present the system model in section 3 and the ray tracing simulation method in section 4. The proposed DACM is presented in section 5, fol-

lowed by the simulation results in section 6. In section 7 and 8, we present a guideline for the model implementation and model verification, and we conclude the paper in section 9.

2. LITERATURE REVIEW

In the existing literature, standard models draw great attention since they are regulated and agreed on by organizations across the world [8, 9, 10]. Among all the standard models, cooperation in science and technology (COST) models are widely accepted. The different COST channel models e.g. COST 207, COST 231, COST 259, COST 273 and COST 2100 were developed to address specific objectives in various application fields [8, 9, 10, 11, 12].

COST 259 has a three-layered framework structure, specifying 13 radio propagation environments considered in the analysis of performance in wireless systems [8, 13]. It clusters MPCs in the delay domain and models the channel by distance-dependent path loss, shadowing fading, and power-delay-angular-profile. Adopting the hierarchy of modeling concepts similar to COST 259, the COST 273 model provides two significant achievements: 1) New scenarios for multiple-input multiple-output (MIMO) are defined; and 2) the clusters are considered differently i.e., apart from local clusters and single clusters, twin clusters are introduced to simulate multiple-bounce interactions [9]. Moreover, the COST 2100 model extended the COST 273 model by the novel developments of the polarization of the channel, dense multipath components and multi-link aspects [10].

Apart from the aforementioned standard models, some other directional models widely adopted by researchers include analytical models, stochastic models and ray tracing models [14]. Analytical models mathematically describe the channel without considering the specific geography of the environment, such as the independent and identically distributed (i.i.d.) model [15] and the Kronecker model [16]. Stochastic models characterize the radio propagation between transmitters and receivers by using stochastic scatterings [3, 17]. Most of them are geometry-based models but are not limited to a specific site. The COST models mentioned above are also stochastic models. The last classification, ray tracing models, highly depend on the radio propagation environment with a limited range of validity. However, ray tracing models can extract the propagation parameters (path loss, DOD, DOA, and so forth) accurately [18, 19].

Although there are plenty of directional channel models characterizing the propagation from various perspectives, some papers focused on the delay or delay-DOA domain [3, 8, 9], while some papers considered a non-clustering DOA domain [20, 21]. However, the number of papers focusing on the azimuth DOA clusters and the cluster power profile are limited. By contrast, our paper captures the features of the azimuth DOA in clusters. In our proposed model, the clustered DOA features are extracted independently from the delay or other channel parameters. Therefore, our model is in a relatively compact form and focuses on the azimuth DOA domain.

3. SYSTEM MODEL

In this section, we present the transmitter and the receiver system model considering only one base station (BS), and multiple mobile stations (MS). Additionally, we illustrate the virtual city models used in the RTS.

3.1 Transmitter and receiver system model

A basic system layout model is shown in Fig. 1. We consider an omnidirectional transmitter as the BS, located at $\mathbf{L}_{\text{BS}} = [\text{x}_b, \text{y}_b]$ and N MS randomly and uniformly placed within the area, located at fixed positions $\mathbf{L}_{\text{MS}} = [\text{x}_n, \text{y}_n]$, $n = 1, ..., N$. The height of the BS is h_{BS}, and all the MS have an identical height of h_{MS}. Such a system layout is able to capture the propagation features from 360° at various distances. We also propose a local coordinate system for each MS in section 4, and the electromagnetic properties of the simulated BS and MS can be found in section 6.

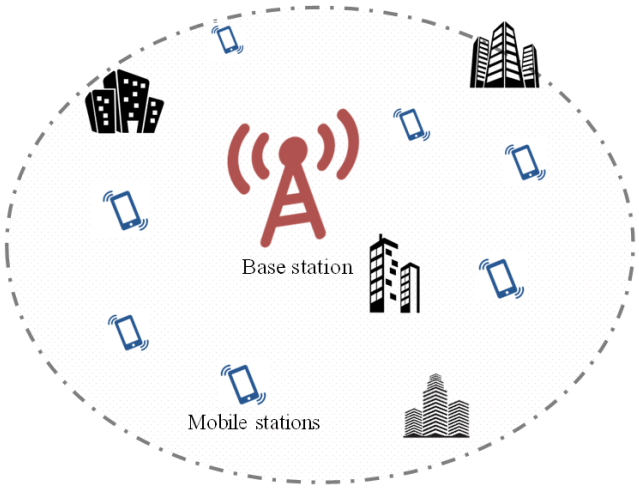

Fig. 1 – System model. The station at the center in red is the base station, and the devices in blue are the mobile stations.

3.2 Virtual urban scenario

Different types of environments have a significant impact on the channel model. For the typical urban scenario we are interested in, it has dense buildings with a relatively small number of large open areas like lakes and parks. Although there is some afforestation in the urban environment, it is out of proportion with buildings. Apart from these aforementioned urban features associated with the building layout, another key factor taken into consideration is the materials of the buildings. The reason is that the materials affect the electrical conductivity and resistivity, leading to a significant impact on the electromag-

netic (EM) propagation. In our RTS, we set the building material as one-layer concrete and the terrain as wet earth. For simplicity, we consider a flat terrain and neglect the afforestation, which is acceptable since it is a typical urban environment. As for the building layout, we follow the Recommendation document proposed by the International Telecommunication Union (ITU) [22]. Three parameters, U_α, U_β, and U_γ detailed in Table 1 are used to generate a virtual random city model. The PDF of the building height follows a Rayleigh distribution [22]

$$f_{\mathrm{h}}(h) = \frac{h \exp(\frac{-h^2}{2U_\gamma^2})}{U_\gamma^2} \qquad (1)$$

where h is the building height in meters.

Table 1 – Parameters for generating a virtual random city model

U_α	Ratio of land area covered by buildings to total land area (dimensionless)
U_β	Mean number of buildings per unit area (buildings/km^2)
U_γ	A variable scaling the building height PDF, defined by a Rayleigh distribution given by *(1)* (dimensionless)

Fig. 2 shows a Manhattan grid layout for the software-generated city. Cubic buildings are uniformly distributed within a square area with side length S m. All buildings share the same square cross-section, $B \times B$ m^2, and fixed street width W m. Both B and W can be obtained from U_α and U_β as $B = 1000\sqrt{\frac{U_\alpha}{U_\beta}}$, and $W = \frac{1000}{\sqrt{U_\beta}} - B$ [23].

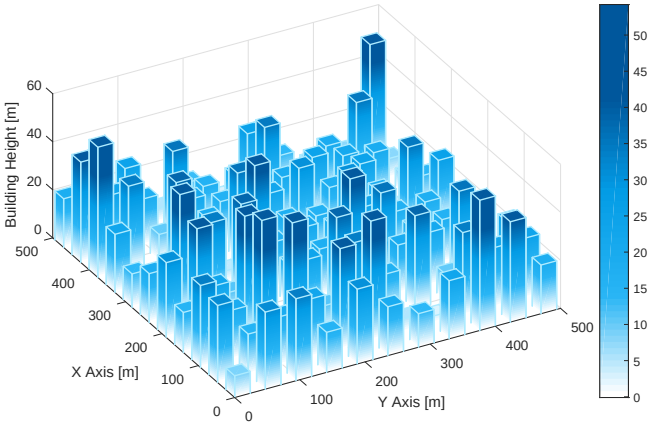

Fig. 2 – A virtual random city generated based on ITU-R parameters.

In this paper, we consider not only software-generated virtual city models but also real urban footprints. The RTS in a real urban environment can give us more practical and reliable insights into the results. We export the footprints and terrain map of the central business district (CBD) area in Melbourne, Australia from online databases [24, 25]. The Melbourne CBD scenario is used for the verification of our proposed directional channel model in section 8.

4. RAY TRACING SIMULATIONS FOR DACM

A ray tracing simulator, Wireless InSite®, is used for the radio propagation modeling in this paper. It predicts radio frequency (RF) signal propagation, as well as EM field in a specific environment and offers a list of output results, including propagation paths between each pair of transmitter and receiver, received signal power, magnitude and phase of E-field, DOA, DOD etc. The major ray propagation mechanisms are line-of-sight(LoS), reflection and diffraction. Scattering is neglected due to the building layout and transmission parameters in this case. Since radio propagation mainly interacts with buildings and terrain in the urban environment, the transmission through objects is also neglected for simplicity. It is reasonable because we are not interested in indoor propagation, nor indoor-to-outdoor propagation. As a result, our simulation involves a mixture of LoS and non-line-of-sight (NLoS) propagation. Fig. 3 shows a pair of BS and MS in Melbourne CBD from the ray tracing simulator as an example. Cubes shaded blue at various height represent the buildings, and the dark green layer at the bottom is the terrain. The green and red cubes are the BS and the MS respectively. In this case, the MS is 600 m away from the BS. The colorful lines are the propagation paths (rays) from BS to MS. Such colors indicate the power level of each ray. Since h_{MS} is identical for all the MS and the terrain is relatively flat in our environment, there is little variation in the elevation angle. As a result, we focus more on the azimuth angle ϕ. The MS itself is the pole of the local angular coordinate system. The LoS direction from the MS to the BS is defined as the angular axis at ϕ = 0°, and ϕ increases counterclockwise from -180° to 180°.

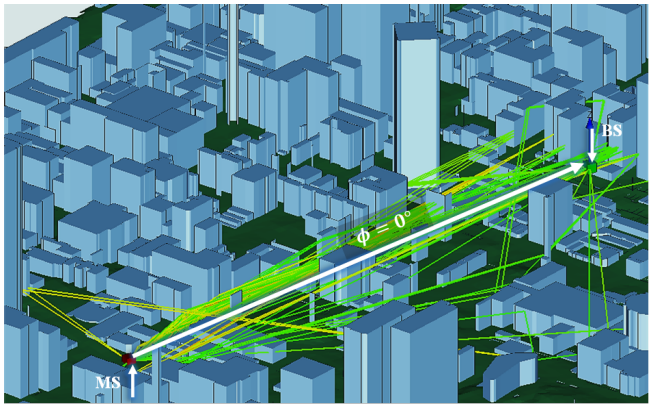

Fig. 3 – The local coordinate system in the ray tracing simulator (simulation environment: Melbourne CBD).

The output data from RTS is further processed by Matlab®. We quantify the parameters for the proposed channel model from curve fitting. The final verification is given by the ray tracing results as well as the numerical results by Matlab® Monte-Carlo simulations. A brief process of the methodology of our DACM is shown in Fig. 4.

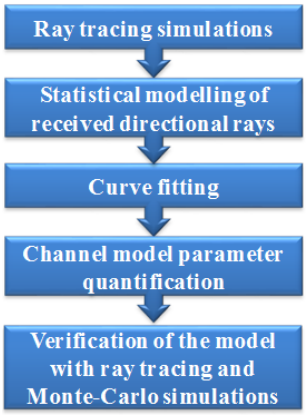

Fig. 4 – The methodology of directional antenna channel modeling.

5. DIRECTIONAL ANTENNA CHANNEL MODELING

In this section, we propose the directional antenna channel model. Firstly, we will introduce the clusters of the rays at the receiver. Then we will present the channel model with three key parameters: 1) the number of clusters and its PMF; 2) the cluster center (in degrees) in the azimuth domain and its PDF; 3) the cluster power ratio (in dBm) and its PDF.

5.1 Clusters of the incident rays

The received signal propagated in a directional antenna channel model can be characterized by the summation of the clusters, and each cluster can be further characterized by the summation of all the rays within the cluster:

$$r(\tau_{\mathrm{i,m}}, \phi_{\mathrm{i,m}}, \beta_{\mathrm{i,m}}) = \sum_{\mathrm{m}=1}^{\mathcal{M}} \underbrace{\sum_{\mathrm{i}=1}^{\mathcal{R}_{\mathrm{m}}} r_{\mathrm{i,m}}(\tau_{\mathrm{i,m}}, \phi_{\mathrm{i,m}}, \beta_{\mathrm{i,m}})}_{r_{\mathrm{m}}(\tau_{\mathrm{i,m}}, \phi_{\mathrm{i,m}}, \beta_{\mathrm{i,m}})} \quad (2)$$

where τ, ϕ and β are the delay, DOA and power ratio of the received signal respectively, the subscript m and i represent the corresponding parameters of the m-th cluster and the i-th ray. The terms $r_{\mathrm{i,m}}(\tau_{\mathrm{i,m}}, \phi_{\mathrm{i,m}}, \beta_{\mathrm{i,m}})$ and $r_{\mathrm{m}}(\tau_{\mathrm{i,m}}, \phi_{\mathrm{i,m}}, \beta_{\mathrm{i,m}})$ represent the received signal of each ray and each cluster, respectively. We define that at one receiver, the cluster number is $\mathcal{M}$, and the number of rays within each cluster is $\mathcal{R}_{\mathrm{m}}$.

Fig. 5 shows an example given by one MS located 600 m away from the BS in a virtual random city environment. In particular, Fig. 5(a), Fig. 5(b) and Fig. 5(c) illustrate the cluster classification considering clustered rays in the ray tracing simulator, the delay domain and the azimuth DOA domain, respectively. As expected, the received rays are clustered in both delay domain and angular domain. The clusters in both domains have some similarities to a certain degree. However, the cluster division in two domains does not always share the exact consistency since multiple complex factors in the scenario are responsible for the result of τ and ϕ. It is common in the existing literature that the authors start analyzing the channel from the delay domain, and the azimuth spread has some correlation with the delay [8, 9]. In this paper, we believe that it is worthy of focusing more on the features of the directionality of the wireless channel.

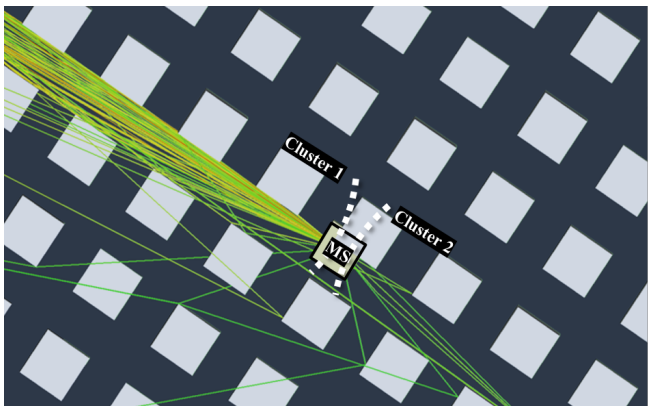

(a) Visualized clustered rays in the ray tracing simulator.

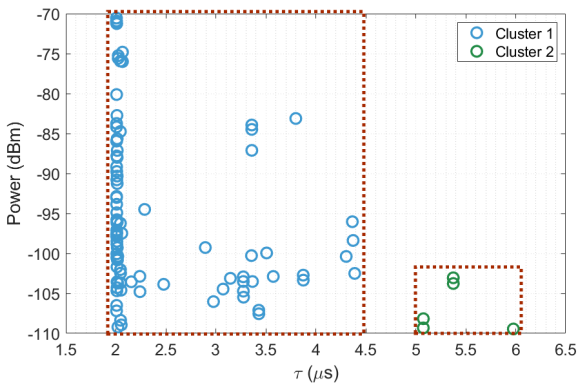

(b) Clustered rays in the delay domain.

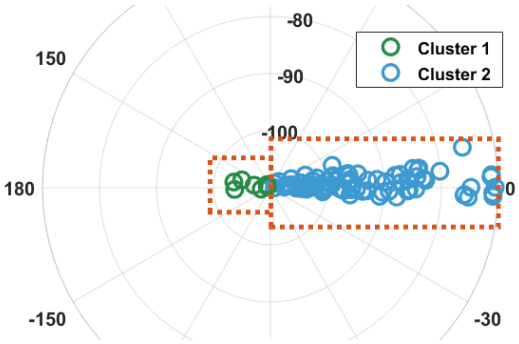

(c) Clustered rays in the azimuth domain.

Fig. 5 – An example of the rays in clusters with respect to τ and ϕ.

To further characterize the clusters of ϕ, we define the cluster gap, ω, as the shortest angular distance between two clusters in degree. In other words, if the DOA of two neighboring rays has a gap greater than ω, these two rays fall into two clusters. Noting that in our system model in section 3, we consider MS located at random positions. However, the final results show that the distance between

MS and BS does not have a significant impact on our results. The main reason is that we set the simulation area as a square with a side length of 1.6 km, and farthest distance from MS to BS is 600 m. The distance variation in our simulation is not very big, but it is enough to cover a reasonable range. In other words, our model is distance-independent, valid for a range of a few hundred meters, such as an outdoor urban microcell scenario. In the following parts of this section, the directional channel model is represented with two carrier frequencies, 2 GHz and 28 GHz, to cover both examples of microwave and mmWave spectrum.

5.2 Number of clusters

Once the cluster gap ω is set, all the rays at one receiver can be grouped into $\mathcal{M}$ clusters in the azimuth domain. $\mathcal{M}$ is characterized by its PMF, $P(\mathcal{M} = i)$, i=1,...,5, presented in Table 2.

Table 2 – Probability mass function of $\mathcal{M}$

$\mathcal{M}$	1	2	3	4	5
2 GHz	0.2496	0.4389	0.2551	0.05419	0.002193
28 GHz	0.3821	0.3836	0.2005	0.03124	0.002588

5.3 Cluster center

To further outline the azimuth feature of the clusters, we introduce cluster center, ϕ_{m}, as the average azimuth of all the rays within the same cluster

$$\phi_{\mathrm{m}} = \frac{\sum_{i=1}^{\mathcal{R}_{\mathrm{m}}} \phi_i}{\mathcal{R}_{\mathrm{m}}} \tag{3}$$

where $\mathcal{R}_{\mathrm{m}}$ is the total number of rays within the same cluster. ϕ_i is the DOA per ray within this cluster in degree. Then based on our RTS, we extract the PDF of ϕ_{m} as a piecewise exponential function,

$$f_\phi(\phi_{\mathrm{m}}) = \begin{cases} a_2 \exp(-b_2(\phi_{\mathrm{m}} + 90)), & -180 \le \phi_{\mathrm{m}} < -90 \\ a_1 \exp(b_1 \phi_{\mathrm{m}}), & -90 \le \phi_{\mathrm{m}} < 0 \\ a_1 \exp(-b_1 \phi_{\mathrm{m}}), & 0 \le \phi_{\mathrm{m}} < 90 \\ a_2 \exp(b_2(\phi_{\mathrm{m}} - 90)), & 90 \le \phi_{\mathrm{m}} < 180. \end{cases} \tag{4}$$

To make *(4)* right continuous and symmetric on $\phi_{\mathrm{m}} = 0$,

$$a_2 = f_\phi(\phi_{\mathrm{m}} = -90) = a_1 \exp(-90 b_1) \tag{5}$$

Table 3 – Parameters of $f_\phi(\phi_{\mathrm{m}})$

f_c	a_1	b_1	b_2
2 GHz	0.005658	0.01340	0.007666
28 GHz	0.007494	0.02485	0.02121

Parameters obtained by curve fitting are presented in Table 3. Noting that due to the curve fitting, we end up with the result for the model such that $\int_{-180}^{180} f_\phi(\phi_{\mathrm{m}}) d\phi_{\mathrm{m}} \approx 1$.

5.4 Cluster power ratio

The power per cluster can be solved by two sub-problems, the total received power, $\mathrm{P_r}$ at the MS, and the power distribution among $\mathcal{M}$ clusters. In this paper, we are more interested in the latter problem. For the first one, based on the specific scenarios, the $\mathrm{P_r}$ calculation can be solved by many widely accepted omnidirectional path loss models in the existing literature, such as the log-normal shadowing model, two-ray model, Okumura–Hata model etc. In this paper, we do not recommend any path loss exponent or shadowing parameters, because the main contribution from us is the directional features of the power at the receiver end. To model the power per cluster, we define a cluster power ratio as

$$\beta_{\mathrm{m}} = \frac{\mathrm{P_m}}{\mathrm{P_r}}. \tag{6}$$

Note that $0 < \beta_{\mathrm{m}} \le 1$, and if $\mathcal{M} = 1$, $\beta_{\mathrm{m}} = 1$. For other cases given $\mathcal{M} > 1$, we find that no matter what the value of $\mathcal{M}$ is, the PDF of β_{m} follows a U-shape distribution, which can be very well fitted by Kumaraswamy distribution [26].

$$K(\beta_{\mathrm{m}}|\mathcal{M}) = \begin{cases} 1, & \mathcal{M} = 1 \\ cd\beta_{\mathrm{m}}^{c-1}(1-\beta_{\mathrm{m}}^{c})^{d-1}, & \mathcal{M} > 1. \end{cases} \tag{7}$$

A summary of c and d parameters conditioned by $\mathcal{M}$ is listed in Table 4. Another important condition of the power ratio is that the summation of all the β_{m} at one MS is 1, $\sum_{\mathrm{m}=1}^{\mathcal{M}} \beta_{\mathrm{m}} = 1$.

Table 4 – Parameters of β_{m}

f_c	$\mathcal{M}=2$		$\mathcal{M}=3$		$\mathcal{M}=4$		$\mathcal{M}=5$	
	c	d	c	d	c	d	c	d
2 GHz	0.17	0.37	0.15	0.45	0.20	0.55	0.03	0.50
28 GHz	0.17	0.37	0.12	0.55	0.05	0.50	0.01	0.55

6. SIMULATION RESULTS

In the RTS, we consider the system models presented in section 3 using the parameters in Table 5.

We generate five realizations of the virtual city models with the same set of U_α, U_β and U_γ, and launch RTS in five such environments to average the randomness. At each MS, we consider the maximum of 100 incident rays. However, the power of some rays can be low, so that they hardly contribute to the total received signal. Therefore, we remove such rays with power below a threshold, $\mathrm{P_{off}}$ = -150 dBm. The RTS returns ϕ_{i} in the output files and the

Table 5 – Simulation parameters

ITU-R urban parameters	U_α = 0.3 U_β = 500 buildings/km^2 U_γ = 15
Virtual city side length (S)	1600 m
BS height (h_{BS})	30 m
MS height (h_{MS})	1.5 m
Number of MS (N)	3771
BS transmit power (P_t)	20 dBm
Carrier frequency (f_c)	2 GHz, 28 GHz
Cut-off power (P_{off})	-150 dBm
Max rays per MS ($\mathcal{R}^{\text{MAX}}$)	100
Cluster gap (ω)	50°

data can be clustered by sophisticated algorithms such as hierarchical clustering once the shortest distance ω is set up. Then $\mathcal{M}$ and ϕ_m can be determined consequently. Finally when taking all MS into consideration, $P(\mathcal{M})$ and $f_\phi(\phi_\text{m})$ can be obtained by calculating their PMF and PDF respectively. Fig. 6 shows the comparison of the directional channel model and the RTS results regarding ϕ_m. Adjustments on the curve fitting parameters have been made to have $f_\phi(\phi_\text{m})$ symmetric on ϕ_m = 0 and right continuous. The final step is to model the power per cluster. We use the E-field strength per ray from RTS to solve this problem. The total received power per MS is $\text{P}_\text{r} = \sum_{i=1}^{\mathcal{R}} P_i$, and the power per cluster is $\text{P}_\text{m} = \sum_{i=1}^{\mathcal{R}_\text{m}} P_i$ [27], where P_i is the time averaged received power in watts of the i-th ray, calculated by the E-field components:

$$P_i = \frac{\lambda^2 F}{8\pi\eta_0}\left|E_{\theta,i} + E_{\phi,i}\right|^2 \tag{8}$$

$$= \frac{\lambda^2 F}{8\pi\eta_0}\left|M_{\theta,i}e^{j\psi_{\theta,i}} + M_{\phi,i}e^{j\psi_{\phi,i}}\right|^2. \tag{9}$$

where $E_{\theta,i}$ and $E_{\phi,i}$ are the θ and ϕ components of E-field of the i-th ray, M and ψ are the magnitude and the phase of the ray, λ is the wavelength, η_0 is the impedance of free space (377 Ω) and F is the overlap of the frequency spectrum of the transmitted waveform and the spectrum of the frequency selectivity of the receiver [27]. The power ratio in *(6)* can be rewritten as:

$$\beta_\text{m} = \frac{\sum_{i=1}^{\mathcal{R}_\text{m}}\left|M_{\theta,i}e^{j\psi_{\theta,i}} + M_{\phi,i}e^{j\psi_{\phi,i}}\right|^2}{\sum_{i=1}^{\mathcal{R}}\left|M_{\theta,i}e^{j\psi_{\theta,i}} + M_{\phi,i}e^{j\psi_{\phi,i}}\right|^2}. \tag{10}$$

Two examples of the curve fitting for $K(\beta_\text{m})$ given $\mathcal{M} = 2$, f_c = 2 GHz and $\mathcal{M} = 3$, f_c = 28 GHz are shown in Fig. 7.

7. DACM IMPLEMENTATION STEPS USING SOFTWARE TOOLS

The proposed directional channel model in this paper enables readers to calculate the distributed azimuth and power in clusters. Such information can be helpful when directional features play an important role in the design and analysis of the wireless channel, for example,

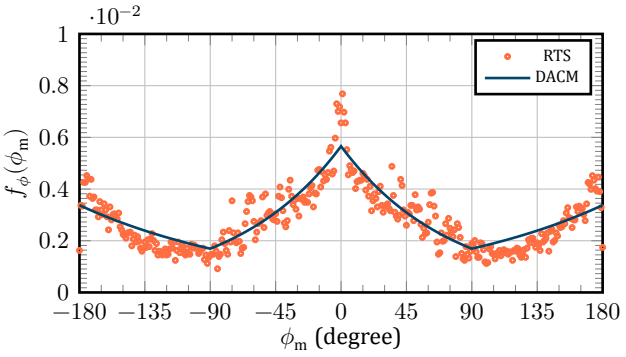

(a) f_c = 2 GHz

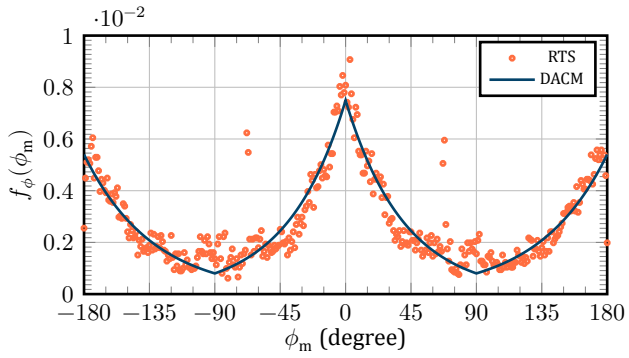

(b) f_c = 28 GHz

Fig. 6 – The curve fitting of $f_\phi(\phi_\text{m})$ at 2 GHz and 28 GHz.

some 5G direction-based applications. We summarize the model in two phases, the directionality of the clusters and the power distribution. The guideline for the model implementation is in Algorithm 1.

Algorithm 1 DACM implementation steps

1: Get system set-up parameters, f_c, N
2: **for each** Receiver n **do**
3: Get number of clusters $\mathcal{M}$, following the PMF in Table 2
4: **for all** m $\in \mathcal{M}$ **do**
5: Get ϕ_m following *(4)*
6: **Condition:** MAX$(\phi_\text{m} - \phi_{\text{m-1}}) \leq \omega$, m $= 2...\mathcal{M}$
7: Get β_m following *(7)*
8: **Condition:** $\sum_{\text{m}=1}^{\mathcal{M}} \beta_\text{m} = 1$
9: $\text{P}_\text{m} \leftarrow \beta_\text{m}\text{P}_\text{r}$
10: **end for**
11: **end for**

8. DACM VERIFICATION

To verify our model, we propose two methods, ray tracing simulated verification by Wireless Insite® and numerically simulated verification by Monte-Carlo simulations. For the former method, we consider both virtual city (VC) models generated by Matlab® and an actual Melbourne CBD footprint imported from online databases [24, 25]. The system model for the verification follows the same set-up as section 3. Then we choose N = 500 receivers uniformly from RTS set-up to join the verifying calcula-

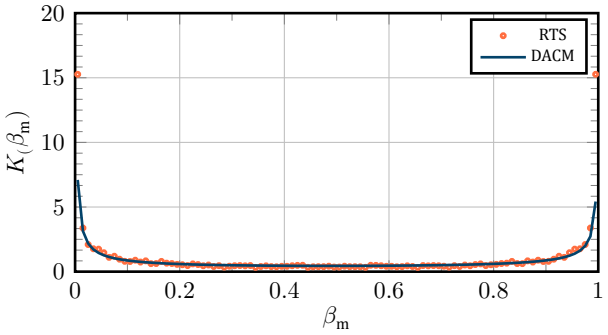

(a) $\mathcal{M} = 2$, f_c = 2 GHz

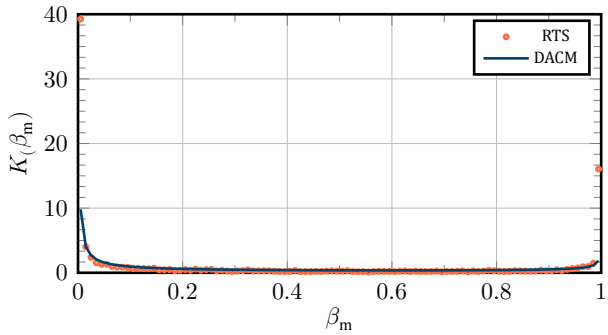

(b) $\mathcal{M} = 3$, f_c = 28 GHz

Fig. 7 – Examples of the curve fitting for $K(\beta_m)$.

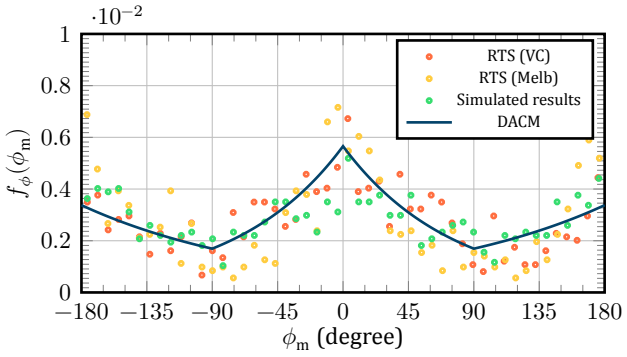

(a) Verification on ϕ_m, f_c = 2 GHz

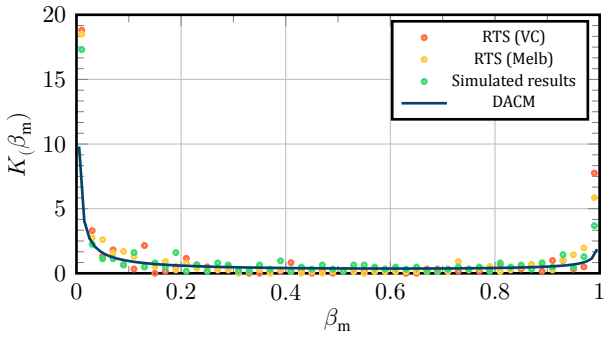

(b) Verification on β_m, $\mathcal{M} = 3$, f_c = 28 GHz

Fig. 8 – Examples of the channel model verification on ϕ_m and β_m.

tion. For the latter method, we simulate the channel following Algorithm 1. The receiver number is also N and the simulation follows the steps in section 7. A comparison of these verifying cases, RTS (VC), RTS (Melb), simulated model and the channel model can be found in Fig. 8. In both of the sub-figures, the scattered dots are the verification results, and the colors, red, yellow and green represent the RTS in a virtual city, the RTS in Melbourne CBD and the numerical results respectively. The solid blue line is the proposed directional channel model. The carrier frequencies are 2 GHz for Fig. 8(a) and 28 GHz for Fig. 8(b). The three verification cases match the model very well in both figures. Actually, we have verified every case, including ϕ_m, β_m conditioned by each $\mathcal{M}$ at two frequencies. All the cases have shown a high level of matching. However, only two examples are depicted in this paper.

9. CONCLUSION

In this paper, we presented a statistical clustering DACM for a general urban scenario. It can benefit the directional wireless network design, optimization and utilization in substance since the channel features can be estimated by merely a few distance-independent probability distribution parameters. The model is proposed in three key aspects, the number of clusters, the cluster center distribution and the cluster power ratio distribution at two carrier frequencies, 2 GHz and 28 GHz. We have concluded that for both frequencies, these three parameters share similar features but with notable differences. Compared with 2 GHz, 28 GHz tends to bring relatively equal probability of the cluster number if $\mathcal{M} \leq 3$, but these clusters are more concentrated at the LoS direction, and the power distribution is more uneven. Future works can be extended from the 2D model to a 3D air-to-ground channel model, which brings more interest to the elevation angle. Also, the clustering algorithm and the modeling of the root mean square delay will be studied to make the DACM more completed.

REFERENCES

[1] NGMN Alliance, "NGMN 5G white paper," accessed 2019-07-17. [Online]. Available: https://www.ngmn.org/work-programme/5g-white-paper.html

[2] Z. Li, K. Magowe, A. Giorgetti, and S. Kandeepan, "Blind localization of primary users with sectorial antennas," in *IEEE International Conference on Communications Workshops (ICC Workshops)*, Kansas City, MO, USA, May 2018, pp. 1–6.

[3] R. T. Rakesh, G. Das, and D. Sen, "An analytical model for millimeter wave outdoor directional non-line-of-sight channels," in *IEEE International Conference on Communications (ICC)*, Paris, France, May 2017, pp. 1–6.

[4] M. Shafi, J. Zhang, H. Tataria, A. F. Molisch, S. Sun, T. S. Rappaport, F. Tufvesson, S. Wu, and K. Kitao, "Microwave vs. millimeter-wave propagation channels: Key differences and impact on 5G cellular systems,"

IEEE Communications Magazine, vol. 56, no. 12, pp. 14–20, December 2018.

[5] E. Anderson, G. Yee, C. Phillips, D. Sicker, and D. Grunwald, "The impact of directional antenna models on simulation accuracy," in *IEEE International Symposium on Modeling and Optimization in Mobile, Ad Hoc, and Wireless Networks*, Seoul, Korea, Jun 2009, pp. 1–7.

[6] Z. Yun and M. F. Iskander, "Ray tracing for radio propagation modeling: Principles and applications," *IEEE Access*, vol. 3, pp. 1089–1100, 2015.

[7] R. He, B. Ai, A. F. Molisch, G. L. Stuber, Q. Li, Z. Zhong, and J. Yu, "Clustering enabled wireless channel modeling using big data algorithms," *IEEE Communications Magazine*, vol. 56, no. 5, pp. 177–183, May 2018.

[8] A. F. Molisch, H. Asplund, R. Heddergott, M. Steinbauer, and T. Zwick, "The COST 259 directional channel model-part I: Overview and methodology," *IEEE Transactions on Wireless Communications*, vol. 5, no. 12, 2006.

[9] A. F. Molisch, H. Hofstetter, and et al., "The COST 273 channel model," New York, NY, USA, 2006.

[10] L. Liu, C. Oestges, J. Poutanen, K. Haneda, P. Vainikainen, F. Quitin, F. Tufvesson, and P. D. Doncker, "The COST 2100 MIMO channel model," *IEEE Wireless Communications*, vol. 19, pp. 92–99, December 2012.

[11] COST 207 Management Committee, *COST 207: digital land mobile radio communications*. Commission of the European Communities, 1989.

[12] E. Damosso *et al.*, "Digital mobile radio: Cost 231 view on the evolution towards 3rd generation systems," *European Commission*, 1998.

[13] H. Asplund, A. A. Glazunov, A. F. Molisch, K. I. Pedersen, and M. Steinbauer, "The COST 259 directional channel model-part II: macrocells," *IEEE Transactions on Wireless Communications*, vol. 5, no. 12, 2006.

[14] P. Almers, E. Bonek, A. Burr, N. Czink, M. Debbah, V. Degli-Esposti, H. Hofstetter, P. Kyösti, D. Laurenson, G. Matz *et al.*, "Survey of channel and radio propagation models for wireless mimo systems," *EURASIP Journal on Wireless Communications and Networking*, vol. 2007, no. 1, p. 019070, 2007.

[15] E. Telatar, "Capacity of multi-antenna Gaussian channels," *European transactions on telecommunications*, vol. 10, no. 6, pp. 585–595, 1999.

[16] H. Ozcelik, M. Herdin, W. Weichselberger, J. Wallace, and E. Bonek, "Deficiencies of 'kronecker' MIMO radio channel model," *Electronics Letters*, vol. 39, no. 16, pp. 1209–1210, 2003.

[17] J. Chen, F. Bin, X. Ge, Q. Li, and C. X. Wang, "A dual-directional path-loss model in 5G wireless fractal small cell networks," in *IEEE International Conference on Communications*, 2017, pp. 1–6.

[18] N. Lertsirisopon, G. S. Ching, M. Ghoraishi, J. Takada, I. Ida, Y. Oishi *et al.*, "Directional channel characteristics from microcell measurement and simulation," in *Proceedings of Asia-Pacific Microwave Conference*, Bangkok, Thailand, 2007, pp. 1–4.

[19] D. Green, Z. Yun, and M. F. Iskander, "Propagation characteristics in urban environments," in *IEEE/ACES International Conference on Wireless Information Technology and Systems and Applied Computational Electromagnetics,*, Honolulu, HI, USA, 2016, pp. 1–2.

[20] H. Luo and Y. I. Wu, "A wireless channel model for the multipaths' doa distribution, assuming directional antennas at transmitter and receiver," in *IEEE International Conference on Consumer Electronics*, Taiwan, Province of China, June 2015, pp. 414–415.

[21] A. Y. Olenko, K. T. Wong, and M. Abdulla, "Analytically derived TOA-DOA distributions of uplink/downlink wireless-cellular multipaths arisen from scatterers with an inverted-parabolic spatial distribution around the mobile," *IEEE Signal Processing Letters*, vol. 12, no. 7, pp. 516–519, July 2005.

[22] Radiocommunication Sector of ITU, "Recommendation p.1410 : Propagation data and prediction methods required for the design of terrestrial broadband radio access systems," International Telecommunication Union, Tech. Rep. Recommendation P.1410, 2003.

[23] A. Al-Hourani, S. Kandeepan, and A. Jamalipour, "Modeling air-to-ground path loss for low altitude platforms in urban environments," in *IEEE Global Communications Conference*, Austin, TX, USA, Dec 2014, pp. 2898–2904.

[24] "ELVIS - Elevation - Foundation Spatial Data," accessed 2019-06-17. [Online]. Available: http: //elevation.fsdf.org.au/

[25] "AURIN Portal," accessed 2019-06-17. [Online]. Available: https://portal.aurin.org.au/

[26] P. Kumaraswamy, "A generalized probability density function for double-bounded random processes," *Journal of Hydrology*, vol. 46, no. 1, pp. 79–88, 1980.

[27] *Wireless InSite Reference Manual*, Remcom, November 2017.